Effects of silica nanoparticle addition and PDMS coating on membrane performance and stability in the extraction of aromatic amines

Gilles Van Eygen[a,b,c,*], Amaury Gilles[b], Julieta Garcia-Chirino[c], Nilay Baylan[c,d], Anita Buekenhoudt[a], Bart Van der Bruggen[c], Patricia Luis[b,e]

a Unit Separation and Conversion Technology, Vlaamse Instelling voor Technologisch Onderzoek (VITO NV), Boeretang 200, 2400 Mol (Belgium)

b Materials & Process Engineering (IMAP), UCLouvain, Place Sainte Barbe 2, B-1348 Louvain-la-Neuve (Belgium)

c Process Engineering for Sustainable Systems (ProcESS), KU Leuven, Celestijnenlaan 200f, 3001 Leuven (Belgium)

d Department of Chemical Engineering, Istanbul University-Cerrahpaşa, Avcılar, 34320, Istanbul, Turkey

e Research & Innovation Centre for Process Engineering (ReCIPE), Place Sainte Barbe 2, bte L5.02.02, B-1348 Louvain-la-Neuve (Belgium), Tel: +32 (0)10 47 25 87 - Fax: +32(0)10 47 40 28

* Corresponding author: gilles.vaneygen@vito.be

Keywords — coatings, supported liquid membranes, extraction technology, aromatic amines.

Graphical abstract

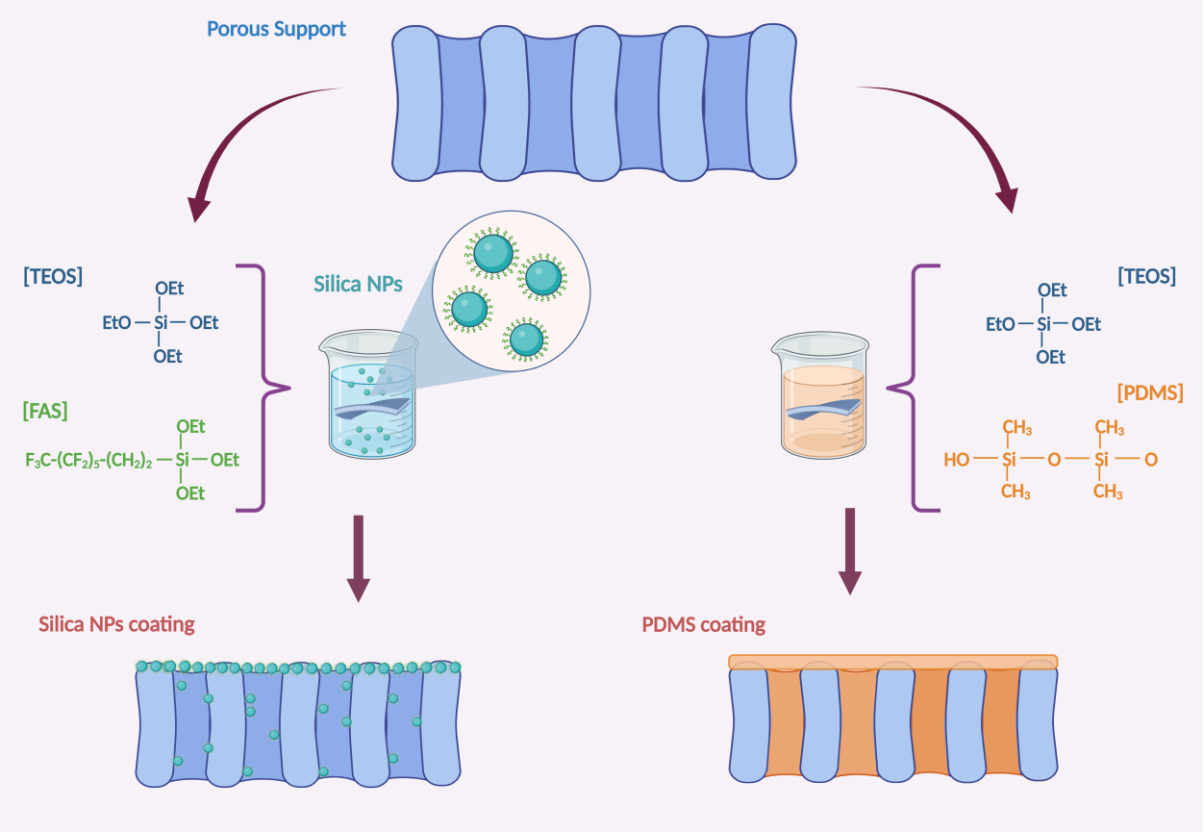

Created in BioRender. García, J. (2024) BioRender.com/e49q927

Abstract

This study investigates novel strategies to improve membrane performance and stability in the extraction of aromatic amines for chiral amine production. The effects of silica nanoparticle addition and polydimethylsiloxane (PDMS) coating were explored, with a focus on the selective extraction of α-methylbenzylamine (MBA) and 1-methyl-3-phenylpropylamine (MPPA) from isopropyl amine (IPA). This work introduces a comparative analysis between open and tight membrane extraction (ME) systems, with and without the ionic liquid (IL) $[P_{6,6,6,14}][N(Tf)_2]$. The results reveal that PDMS creates a uniform and dense coating, particularly on PTFE and PVDF supports, while silica nanoparticle coatings were less stable, retaining only 50% of nanoparticles after ME testing. A PDMS-coated PTFE membrane achieved significantly higher solute fluxes of 1.12 ± 0.01, 1.66 ± 0.02, and 0.36 ± 0.08 g/(m²h) for MBA, MPPA, and IPA, respectively, compared to an IL-wetted PTFE membrane, which was found to have fluxes of 0.60 ± 0.06, 1.01 ± 0.04, and 0.33 ± 0.10 g/(m²h) for the same solutes. A reduction in the pore size of the PTFE support further increased the fluxes to 1.74 ± 0.28, 2.75 ± 0.25, and 0.45 ± 0.08 g/(m²h) for MBA, MPPA, and IPA, respectively, achieving selectivity values of 3.83 ± 0.65 for MBA/IPA and 6.24 ± 0.88 for MPPA/IPA. Although IL impregnation marginally improved selectivity, it caused a significant reduction in solute fluxes. The PDMS coating retained 92.1% of its mass after 24 hours, while the IL retained 87.2% over the same period. Compared to the tested IL, which presents safety concerns due to its flammability and corrosiveness, PDMS coatings provide a safer and more environmentally friendly alternative, as PDMS is non-toxic and does not bioaccumulate. These findings underscore the superior performance and environmental benefits of novel PDMS-coated membranes in tight ME setups compared to IL-based open ME systems.

Introduction

Chiral amines play a crucial role in drug manufacturing, biologically active compounds, and natural products, comprising 40 to 45% of small pharmaceutical molecules [1]. Notable examples of chiral amine-based pharmaceuticals include berberine (for insulin assimilation [2,3]), sitagliptin (anti-diabetic [4]), formoterol (asthma treatment [5]), and morphine (analgesic [6]). Given their importance, various chiral amine synthesis methods, such as resolution [7], asymmetric hydrogenation [1], organocatalysis [8,9], and biocatalysis [10], have been explored. However, challenges such as the formation of by-products, the use of toxic reagents, and the need for multi-step syntheses, persist. Biocatalytic methods using enzymes, including transaminases and amine dehydrogenases, offer eco-friendly solutions, with transaminases achieving a theoretical yield of 100% [10–13]. However, this yield can only be obtained by shifting the reaction equilibrium, often by using an excess of the amine donor. *In situ* product removal is a promising approach for optimizing amine synthesis by continuously extracting the product [14].

Current *in situ* product removal methods include liquid-liquid extraction (LLE), evaporation, electrodialysis, and membrane separation, with hybrid systems like membrane extraction (ME) offering a particularly promising alternative [15,16]. Membrane extraction uses a membrane acting as a barrier between a donor and receiver phase in which the products are extracted [17]. Two types of ME can be identified: tight ME, which relies on solute-membrane affinity using dense materials, and open ME, which relies on solute-extractant affinity using an immobilised extractant in a porous matrix. The latter is also known as supported liquid membrane (SLM) extraction. Within SLM, the target product is extracted into a liquid membrane (LM) phase and simultaneously removed by the receiver phase, combining extraction and stripping in one step. SLMs use less extractant compared to conventional LLE [14]. The main challenge for the use of SLMs is their short membrane lifetime due to the instability of the LM phase [18]. Since solvent loss directly impacts both environmental sustainability and process efficiency, addressing these stability challenges is crucial.

Various approaches have been explored to improve the performance and stability of SLMs. One of the simplest methods is intermittent re-impregnation of the liquid membrane phase. However, this strategy does not tackle the inherent instability of the SLMs. Continuous re-impregnation by dispersing the liquid membrane phase into one of the circulating phases helps maintain performance but leads to contamination of these phases [19–23]. Alternatively, gelation of the liquid membrane phase using hydrogels, organogels, or ionogels could provide stability, although ionogels often suffer from weak mechanical properties [24–26]. Surface modifications, such as hydrophobization with nanoparticles or polymer coatings, offer further enhancement. Hydrophobic nanoparticles improve SLM performance for specific separations, such as cationic dyes [27], while polymeric coatings enhance stability and efficiency in processes like phenol extraction, metal ion recovery, and nitrate removal [28–30]. Coating membranes with hydrophobic nanoparticles or fluoro-containing silica nanoparticles has also yielded superhydrophobic properties, demonstrating significant potential for improving SLM functionality and durability in separation applications [31].

Despite the variety of methods proposed to improve SLM stability, the literature lacks a comprehensive comparison of these strategies [32]. To this end, the current work explores two novel approaches to enhance the stability and sustainability of SLM processes, focusing on the selective separation of the aromatic amines α-methylbenzylamine (MBA) and 1-methyl-3-phenylpropylamine (MPPA) from isopropyl amine (IPA). MBA is a cost-effective chiral molecule used in enantiomerically pure compounds, chiral ligands, and organocatalysts, while MPPA is a precursor for the antihypertensive drug dilevalol [14,33,34]. A standard SLM process using the ionic liquid [$P_{6,6,6,14}$][$N(Tf)_2$]) as the stable and selective extractant was used as the benchmark. This benchmark is then compared with the effects of adding hydrophobic silica nanoparticles and applying PDMS-based silica coatings. Novel support modifications were characterized using water contact angle measurements, SEM-EDS, and FTIR analyses to evaluate wettability, composition, and functionality. The prepared supports were then used for both open and tight ME, *i.e.*, with or without the addition of the ionic liquid [$P_{6,6,6,14}$][$N(Tf)_2$]) as the selective extractant[14,33,34]The support performance was evaluated based on stability, selectivity, and solute fluxes.

2. Materials and methods

2.1 Chemicals and materials

The feed and strip buffers for the membrane extraction experiments were prepared using the following chemicals: phosphoric acid (85%, VWR), sodium dihydrogen phosphate (≥ 98%, VWR), sodium carbonate (≥ 99.9%, Merck Life), and sodium bicarbonate (A.R., Fisher Scientific). The following amines were used: α-methylbenzylamine or MBA (98%, Merck Life), 1-methyl-3-phenyl-propylamine or MPPA (98%, Sigma-Aldrich) and isopropyl amine or IPA (≥ 99.5%, Sigma-Aldrich). A solution for pH adjustment was prepared using sodium hydroxide (≥ 98.5%, VWR).

The ionic liquid trihexyltetradecylphosphonium bis(trifluoromethylsulfonyl)imide or $[P_{6,6,6,14}][N(Tf)_2]$ (≥ 98%, Iolitec) was used for membrane impregnation. The silica nanoparticles were prepared using the following chemicals: tetraethyl orthosilicate or TEOS (100%, Sigma-Aldrich), tridecafluorooctyl triethoxysilane or FAS (97%, Fluorochem), ethanol (≥ 99.8%, Fisher Chemical), and ammonium hydroxide (25%, Fluka Chemie GmbH). The PDMS coating solution was prepared using the following chemicals: hexane (≥ 98%, Carl Roth), tetraethyl orthosilicate or TEOS (100%, Sigma-Aldrich) and poly(dimethylsiloxane) or PDMS (≤ 2 ppm impurities, Sigma-Aldrich) in liquid form. All chemicals were used without further purification. The commercial support materials used in this study are listed in Table 1.

Table 1. Support materials used in this study.

Name	Material	Pore size/nm	Supplier
Tetratex® #1325	PTFE	50	Donaldson
Tetratex® #1301	PTFE	100	Donaldson
Tetratex® #3103	PTFE	450	Donaldson
Tetratex® #6501	PTFE + PP	100	Donaldson
LX	PES	90	Synder Filtration
V0.1	PVDF	100	Synder Filtration

2.2 Membrane preparation, impregnation, and characterisation

The membranes were cut in a circular shape, approximately 6 cm in diameter. The pristine membranes were then weighed using an analytical scale. If the membranes underwent heat treatment for the coating procedure, they were cut in a slightly larger shape, as they shrank during the heating stage.

2.2.1 Nanoparticle synthesis and membrane coating

The silica nanoparticle solution was prepared according to Wang et al. [31], as shown in Figure 1. First, 5 mL TEOS and 8.566 mL FAS (10:1 molar ratio) were added to a beaker containing 25 mL of ethanol.

Then, 6 mL of a 25% ammonium hydroxide solution were added to a second beaker also containing 25 mL of ethanol. This second solution was poured into the first and the resulting mixture was stirred for 12 hours at room temperature. After ultrasonication of the resulting solution for 30 minutes, the membrane was placed in the solution under gentle stirring for 15, 30, or 60 minutes. After dip coating, the membrane was dried with a paper towel and heat treated in an oven for 60 minutes at 110 °C.

The PDMS coating solution was prepared according to Suleman et al. [35], as shown in Figure 1. First, a solution was prepared by adding 20 w/w% PDMS and 1 w/w% TEOS to 100 mL of hexane. The solution was mixed until a homogeneous mixture was obtained. The membrane was then placed in the solution under gentle stirring for 15, 30, or 60 minutes. After dip coating, the membrane was dried with paper and heat treated in an oven for 45 minutes at 120 °C.

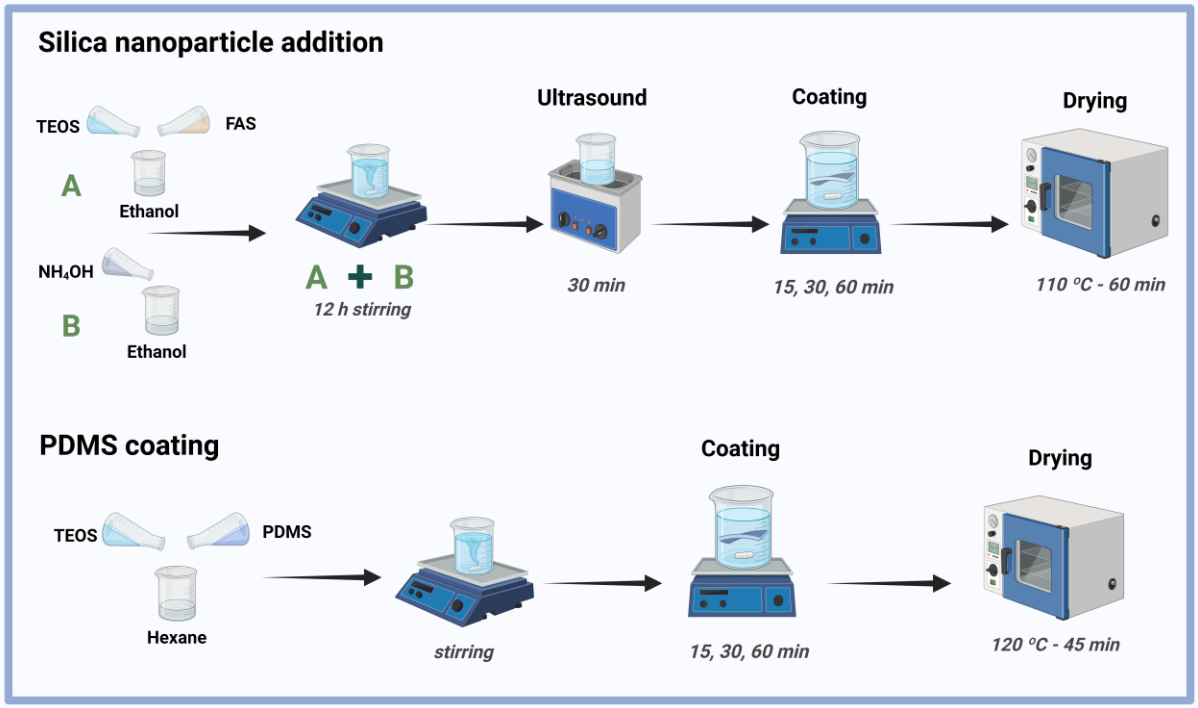

Figure 1. Schematic diagram for the membrane preparation by the addition of silica nanoparticles and PDMS coating. Created in BioRender. García, J. (2024) BioRender.com/m45i707.

2.2.2 Membrane impregnation

For the membrane impregnation, a setup with a Büchner funnel and a vacuum flask connected to a vacuum pump (MPC 201E, ILMVAC GmbH) was used. A support (#6501, see Table 1) was placed in the Büchner funnel to prevent mechanical degradation of the membrane. The circular membrane was then placed on the filtration paper and evenly spread out. The vacuum pump was turned on, and the solvent was gradually added to the membrane using a pipette. The solvent was distributed over the entire membrane surface with a lab spatula. The impregnation time lasted 45 minutes. Afterwards, the membrane was patted with a paper towel to remove any residual solvent.

The membranes were weighed with an analytical scale at each stage: pristine after cutting, after dip coating and/or solvent impregnation, and after ME testing. To quantify the success of the coating and impregnation procedures, two parameters were defined, *i.e.*, the coating and wetting efficiency. The coating efficiency was defined as follows:

$$\text{Coating efficiency [g/m}^2\text{]} = \frac{m_c^t - m_c^0}{A}$$

in which m_c^0 and m_c^t [g] are the membrane mass before and after the coating procedure, respectively. The membrane surface area was denoted by A [m²]. Similarly, the wetting efficiency was defined as:

$$\text{Wetting efficiency [g/m}^2\text{]} = \frac{m_w^t - m_w^0}{A}$$

in which m_w^0 and m_w^t [g] are the membrane mass before and after the impregnation procedure, respectively. Last, the mass residual was defined to quantify the solvent or coating loss during the ME tests:

$$\text{Mass residual [\%]} = \frac{m_e^t - m_{dry}}{m_e^0 - m_{dry}} \cdot 100$$

in which m_e^0 and m_e^t [g] are the membrane mass before and after the ME test, respectively, and m_{dry} [g] is the dry membrane mass.

2.2.3 Membrane characterisation

Scanning electron microscopy (SEM, FEI NOVA NanoSEM 450) was used for imaging of the membrane surface and cross-section morphology. Energy dispersive X-ray spectra (EDS) were obtained using a Bruker X flash6/60 detector and analysed with the Esprit software. The SEM samples were prepared as follows. For surface imaging, a small piece of material was attached to a stub using double-sided carbon tape. For cross-section imaging, the material was either fractured under liquid nitrogen or cut using a scalpel, parallel to the layer structure to minimize compression. The cross-section samples were then affixed to copper tape for added stability and secured in a special stub using a screw. A thin layer (3 nm) of Pt/Pd (80/20) was sputter-coated on all the surfaces.

The wettability of the modified membranes was analysed using a drop shape analyser (DSA 10 Mk2, Krüss). The membranes were cut into rectangular samples measuring 1 by 3 cm². After cutting, the membranes were taped to the platform of the drop shape analyser using double-sided tape. A droplet of ultrapure water with a volume of 4 µL was then deposited on the membrane surface at a rate of 24.59 µL/min, and the contact angle was measured every second for a total duration of 60 seconds. The data were analysed using the Drop Shape Analysis software. Three repetitions were performed on each membrane to obtain a statistical mean value. Functional groups of the coated membranes were determined by Fourier transform infrared (FTIR) spectroscopy (Spectrum 100 FT-IR, Perkin Elmer).

2.4 Membrane extraction experiments

The feed buffer was prepared by dissolving 7.58 g of sodium carbonate and 10.76 g of sodium bicarbonate in 1000 mL of ultrapure water, under continuous stirring. Then, 500 mg of each amine (MBA, MPPA, and IPA) were added to the solution. The strip buffer was prepared by dissolving 21.98 g of sodium dihydrogen phosphate and 1724 µL of an 85% phosphoric acid solution in 1000 mL of ultrapure water. The pH was measured after all compounds were fully dissolved.

A schematic diagram of the membrane extraction setup is shown in Figure 2. First, the membrane was placed in the membrane contactor, positioned between two rubber O-rings, and secured in a Teflon cell. Next, 250 mL of both the feed and strip buffer were added to the appropriate containers. An RTD thermometer (DIGI-SENSE) was used to monitor the temperature of both solutions continuously, while four diaphragm gauge guards with a manometer (Series 3D, 0-6 bar, EM-Technik) were used to check the pressure of the system. The pumps were started at a flow rate of 10 L/h and the flow rates were checked using two variable-area flow meters with a valve (Masterflex). The solutions were continuously stirred using a magnetic air stirrer. The experiment ran in counter-current mode for 24 hours at room temperature. During each experiment, samples were collected at start-up and at intervals of 1, 3, 6, and 24 hours [36,37].

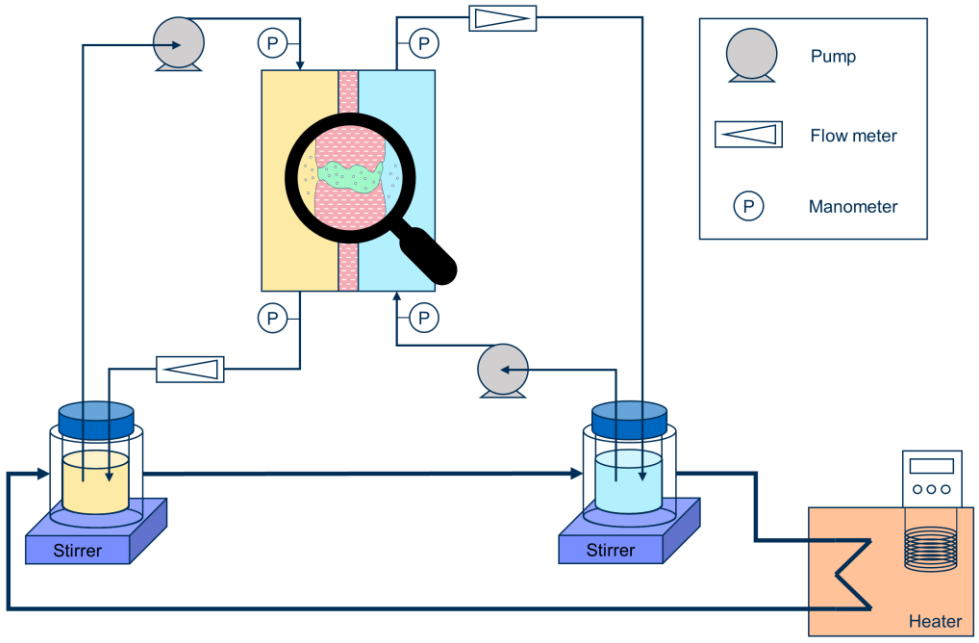

Figure 2. Schematic diagram of the used membrane extraction setup, based on Riedl [38].

HPLC-UVVIS analysis of MBA and MPPA in the samples was conducted using a Shimadzu Prominence-I LC-2030C 3D with gradient elution. Acetonitrile and an 0.1 v% phosphoric acid solution were used as the mobile phases. GC analysis of IPA was performed using a headspace GC-FID Autosystem XL (Perkin Elmer) with helium as the mobile phase and an Rtx-5 Amine column (L = 30 m,

D = 0.25 mm, D_{particle} = 0.50 µm). Before analysis, 200 µL of a 25% sodium hydroxide solution was added to 1 mL of both the feed and strip samples, as IPA can only volatilise at higher pH values.

3 Results and discussion

3.1 Membrane characterisation

3.1.1 Membrane morphology and composition

Effect of coating type

Figure 3 shows the morphology of a PTFE-100 membrane coated for 30 min with PDMS and silica nanoparticles, along with the elemental mapping of both coatings in cross-sectional images, compared with the pristine PTFE-100 membrane. Figure 3b displays the PDMS coating, revealing a dense, uniform membrane surface, compared with the porous structure of the pristine PTFE membrane. The cross-section image highlights a continuous, even layer, suggesting good PDMS incorporation on the substrate. The surface mapping in Figure S1 further confirms the smooth, homogeneous PDMS coating, with a significant silicon (Si) peak (around 25 cps/eV) in the EDS analysis. In contrast, the membrane coated with nanoparticles displays a porous, fibrous structure over the PTFE-100 substrate, as seen in Figure 3c, similar to the pristine membrane. The elemental mapping shows carbon and fluorine as the key elements of the PTFE substrate and confirms the presence of the silica nanoparticles within the layers. The surface mapping in Figure S1 indicates an even distribution of silica nanoparticles, although the Si peak is smaller (around 2 cps/eV), suggesting weaker Si adhesion compared to the PDMS coating.

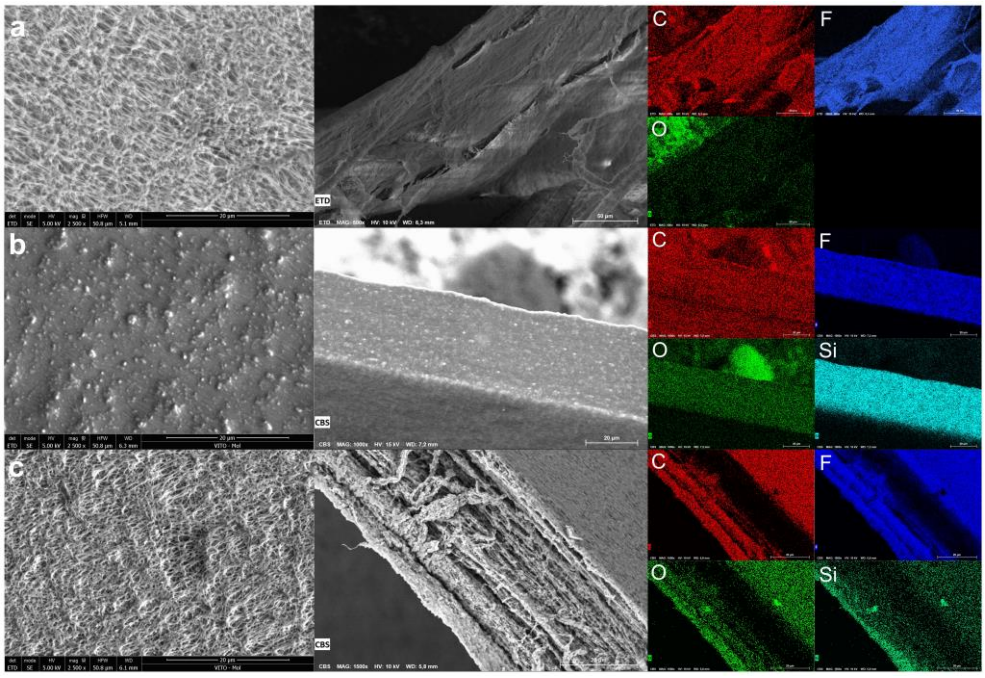

Figure 3. SEM images of the surface, cross-section, and elemental mapping of (a) a pristine PTFE-100 membrane, (b) a PTFE-100 membrane coated with PDMS for 30 minutes, and (c) a PTFE-100 membrane coated with silica nanoparticles for 30 minutes.

Effect of support material

The support material and its properties are key factors in ME applications. Typically, the support is a polymer that can vary in structure, charge, and surface characteristics. For extraction with aqueous solutions, the support must be hydrophobic to serve as a physical barrier between the feed and receiving phase [39]. This study examined three flat-sheet polymeric membranes – polyether sulfone (PES), polyvinylidene fluoride (PVDF), and polytetrafluoroethylene (PTFE) – with varying PTFE pore sizes (see Table 1). The chemical structures of the three polymers are shown in Figure 4.

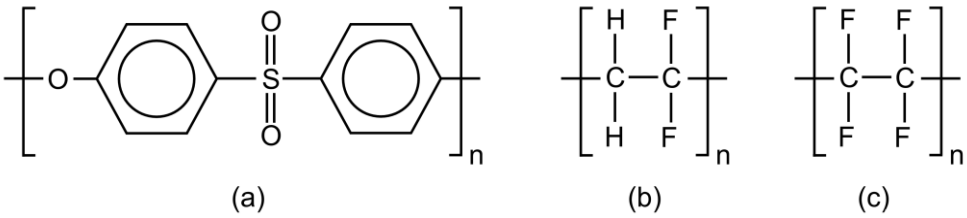

Figure 4. The molecular structures of (a) polyether sulfone (PES), (b) polyvinylidene fluoride (PVDF), and (c) polytetrafluoroethylene (PTFE).

Figure 5 shows the PDMS coating after 30 minutes on a PES-90 and PVDF-100 membrane. The surface of the PES-90 membrane exhibited some deformities with no visible pores, as shown in Figure 5a. Moreover, the cross-section image and mapping reveal a dense top layer and a thicker fibrous layer, which is the polypropylene support. According to the surface mapping in Figure S2a, a homogeneous PDMS incorporation was achieved, and the presence of C, O, and S gives clear evidence of the PES composition. A Si peak of around 6 cps/eV was present, showing less favourable interaction between PDMS and PES, compared to PTFE. The surface of the PVDF-100 membrane, as shown in Figure 5b, exhibited a different interaction with the PDMS coating, resulting in less deformities, again without visible porosity. A clear interface between the PDMS layer and the PVDF-100 is observed in the cross-section image, with an absence of the coating in specific areas based on the EDS images. The mapping of the PVDF-100 surface in Figure S2b confirms a well-distributed PDMS coating with successful silica incorporation, indicated by the large silica peak (around 25 cps/eV).

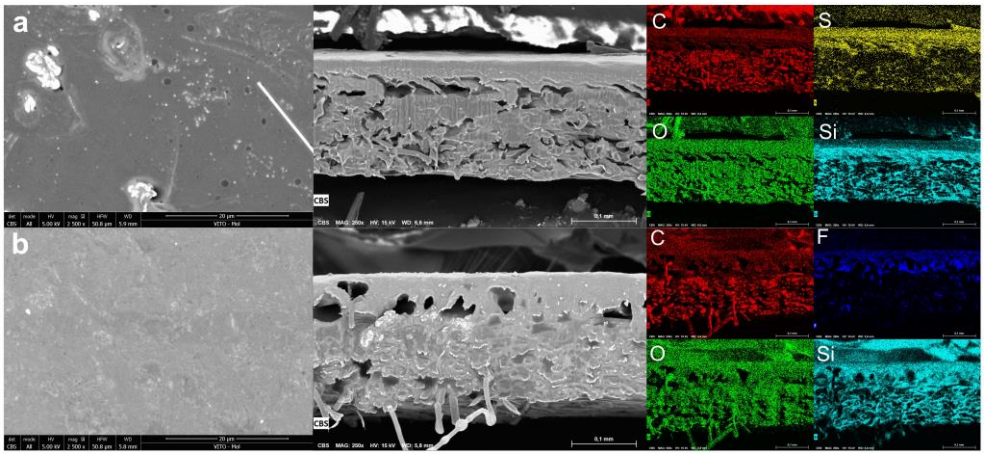

Figure 5. SEM surface, cross-section, and elemental mapping of (a) a PES-90, and (b) a PVDF-100 membrane coated for 30 min with PDMS.

Significant changes are observed after coating the PES-90, PTFE-100, and PVDF-100 membranes with PDMS and silica, as depicted in the FTIR spectrum in Figure 6. In the PES-90 membrane, the PDMS coating introduced new peaks around 2960 cm^{-1} corresponding to -CH_3 stretching [40,41] and strong Si-O-Si vibrations between 1250 – 1000 cm^{-1} [42], confirming the successful deposition of PDMS. For the silica-coated membrane, the disappearance of the -OH stretching (3600 – 3200 cm^{-1}) suggests that the silica layer successfully hydrophobized the membrane surface. PTFE-100 exhibited similar changes with the PDMS coating, as evidenced by the elongation of the peak around 2960 cm^{-1} (CH_3 stretching) and the strong presence of the peak around 800 cm^{-1} corresponding to the Si-CH_3 vibration, indicating significant surface coating [42,43]. The silica-coated PTFE-100 membrane presents a clear Si-O-Si stretching peak around 1100 cm^{-1} [44], confirming silica incorporation on the surface. The C-F characteristic peaks (1350-1200 cm^{-1}) [45] of PTFE appear weak in both coatings, suggesting that the surfaces are dominated either by silica or PDMS. In PVDF-100, the presence of the PDMS coating was confirmed by the Si-O-Si peaks between 1250-1260 cm^{-1} and 1000-1100 cm^{-1} [46]. As for the PVDF-100 silica coating, the strong Si-O peaks near 1100 and 800 cm^{-1} confirmed the presence of silica, and the relative reduction in C-F peaks suggests a more extensive coverage [47].

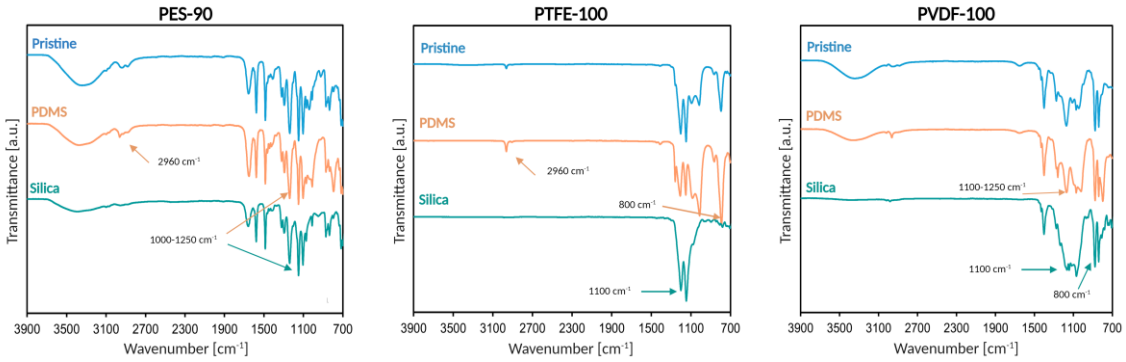

Figure 6. FTIR spectra of pristine membranes and membranes coated with silica nanoparticles and PDMS.

Effect of dip coating time

The effect of coating time was assessed using SEM–EDS imaging, as shown in Figure 7. The results indicate that coating time had minimal impact on the final layer. Additionally, the total layer thickness remains unchanged with varying coating times, as no extra PDMS layer forms on the membrane surface. The PDMS is exclusively and evenly deposited within the internal membrane structure.

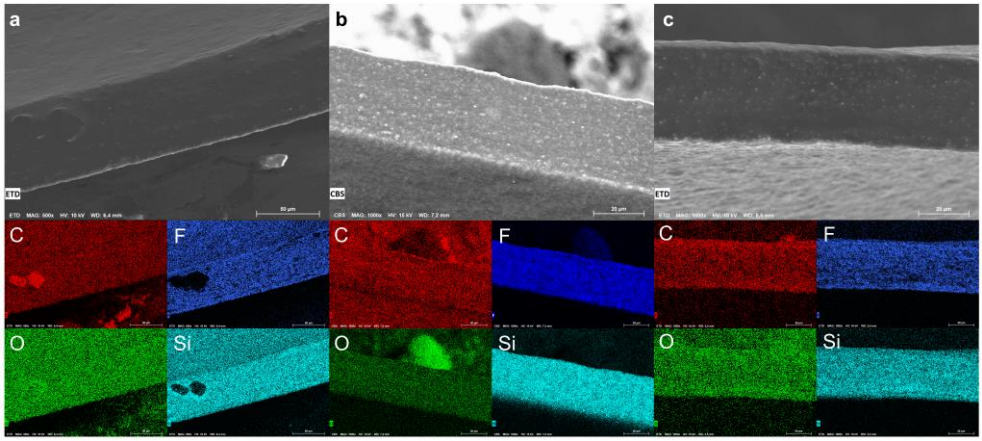

Figure 7. SEM cross-section images and elemental mapping of a PTFE-100 membrane coated with PDMS for a duration of (a) 15 minutes, (b) 30 minutes, and (c) 60 minutes.

3.1.2 Membrane wettability

The effect of the addition of silica nanoparticles and PDMS coating on the different support materials is given in Figure 8a. The pristine membranes show an increasing hydrophobicity in the following order, PES (73.2°) < PVDF (94.1°) < PTFE (128.0°). PES is a hydrophilic molecule due to its molecular structure (see Figure 4), which facilitates hydrogen bonds with water molecules, as both the ether and sulphone groups are polar. On the other hand, PVDF is a semi-crystalline polymer with hydrophobic properties, due to the presence of C-F bonds [48,49]. PTFE also known as Teflon® is highly similar to PVDF but is an even more hydrophobic molecule due to its chemical structure based solely on C-C and

C-F bonds [50,51]. Interestingly, despite variations in the hydrophobicity of the pristine supports, all showed a similar wettability after coating. More specifically, after a 30-minute coating with silica nanoparticles or PDMS, the water contact angle ranged between 124 and 134° for silica nanoparticles and between 91 and 100° for PDMS. This suggests that the wettability of the coated membranes was not significantly affected by the support material, which is logical due to the formation of a dense PDMS layer on the support materials. Moreover, altering the pore size of the support material had little to no impact on the wettability, as shown in Figure 8b.

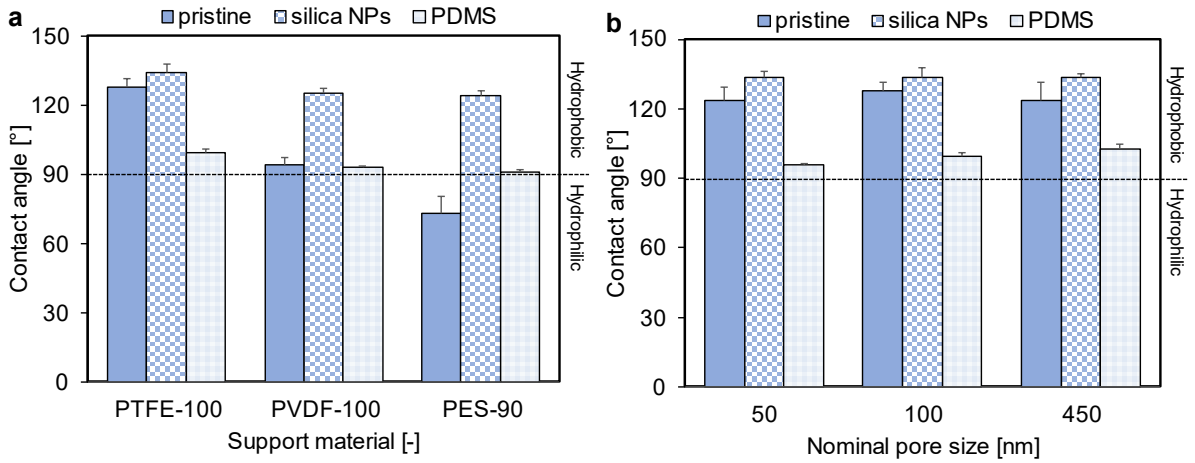

Figure 8. Experimental water contact angle data for (a) various support materials, and (b) PTFE membranes with various pore sizes, both pristine and after a 30 min coating with silica nanoparticles or PDMS.

To analyse the effect of the dip coating time on the membrane wettability, water contact angle measurements were conducted on a PTFE-100 membrane with either a silica nanoparticle or PDMS coating for various coating times (see Figure 9a). The pristine PTFE membrane is already highly hydrophobic with a contact angle of 124.6°, but the silica nanoparticle coating increased its hydrophobicity even more achieving a maximum surface hydrophobicity (CA = 134°) after 30 min, with a subsequent decrease in the water contact angle for longer coating times. On the other hand, the PDMS coating lowered the hydrophobicity of the PTFE membrane to a value of 98.6° after 60 min. No significant differences were observed for varying coating times, although Suleman et al. [35] observed a maximum water contact angle after 30 minutes of dip coating. Moreover, a longer coating time did not result in a thicker PDMS layer, as shown in Figure 7.

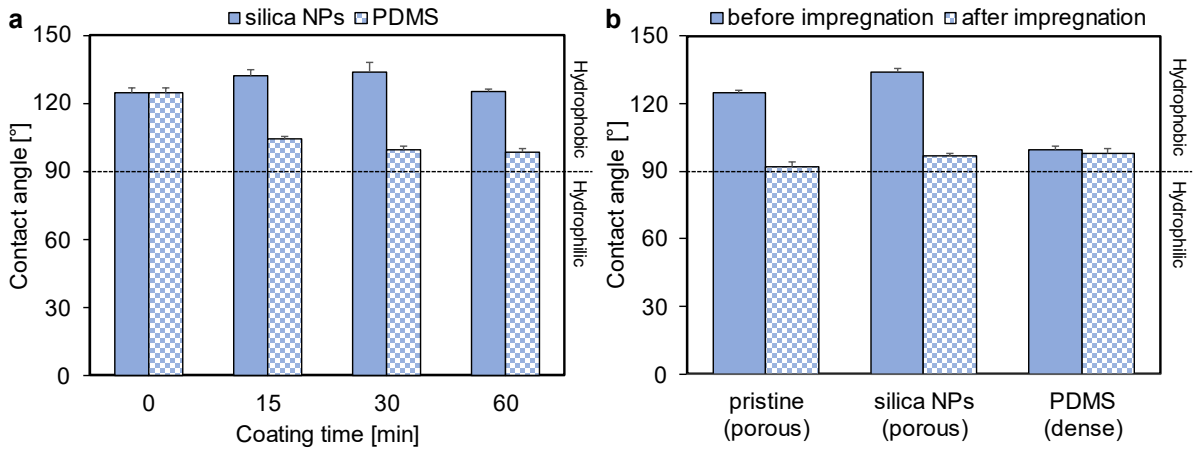

Figure 9. Experimental water contact angle data for a PTFE-100 membrane (a) after various coating times with silica nanoparticles or PDMS, and (b) in its pristine state or after coating with silica nanoparticles or PDMS, both before and after impregnation with the ionic liquid [$P_{6,6,6,14}$][$N(Tf)_2$].

After the coating procedures, the membranes were impregnated with the ionic liquid [$P_{6,6,6,14}$][$N(Tf)_2$] and the water contact angle was measured again. Interestingly, the impregnated membranes showed a similar water contact angle, independent of the used coating procedure, as shown in Figure 9b. For the pristine PTFE membrane, a significant decrease in the water contact angle from 124.6 to 92.1° was observed after impregnation, indicating a considerable change in surface hydrophobicity, possibly due to the IL-water interaction and partial coverage of the PTFE surface. A similar trend can be observed for the membrane coated with silica nanoparticles. Only a slight decrease in water contact angle from 99.6 to 98.0° was found for the PDMS-coated membrane after impregnation, indicating minimal changes in surface hydrophobicity, likely due to better compatibility and less interaction between the IL and the PDMS surface.

3.2 Membrane extraction performance

3.2.1 Coating and wetting efficiency and membrane stability

The success of coating and wetting was determined by their respective efficiency, as outlined in Section 2.2.2. As shown in Figure 10a, the coating efficiency was similar for both the silica nanoparticles and PDMS coating, although the coating with silica nanoparticles showed much more variation. The wetting efficiency significantly decreased when the PTFE membrane was coated with either material, which is logical as the dense coating impairs the penetration of the extractant into the support matrix. Figure 10b presents the mass residuals of the tested membranes, revealing that after ME testing, the PDMS-coated membrane retained 93.0% of its mass, while the silica nanoparticle coated membrane retained only 51.3%, indicating a 50% loss of silica nanoparticles during the process. The pristine IL-impregnated membrane had a mass residual of 87.2%, compared to 81.7% and 89.9% for the silica nanoparticle and

PDMS-coated membranes, respectively. Thus, PDMS coatings showed better stability and even less mass variability.

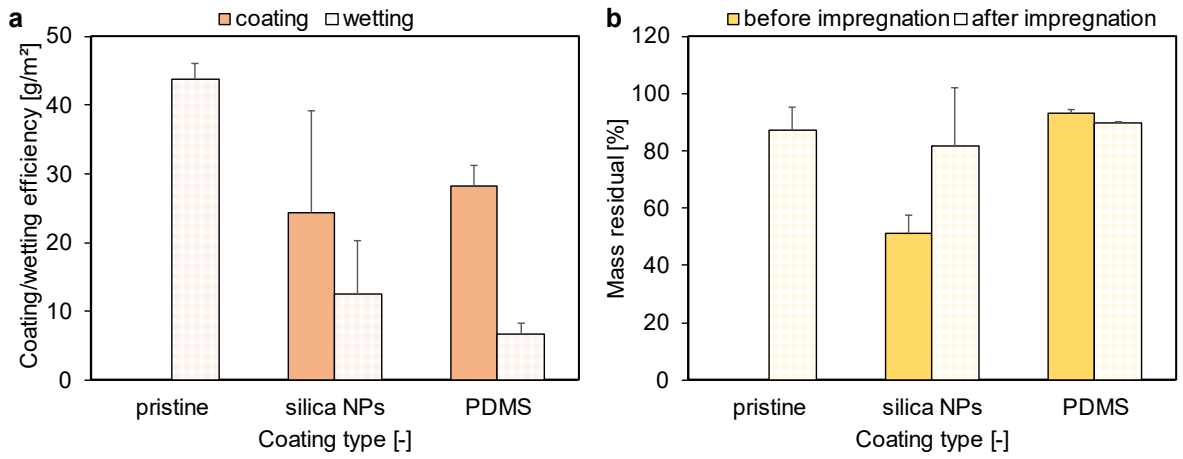

Figure 10. Experimental results of (a) the coating and wetting efficiency, and (b) the mass residual after extraction using a PTFE-100 membrane, either in its pristine state or coated with silica nanoparticles or PDMS, with or without impregnation with the ionic liquid [$P_{6,6,6,14}$][$N(Tf)_2$].

Since the PDMS coating proved to be the most stable, further coating tests were conducted by varying the support material and pore size, as shown in Figure 11. Coating efficiency followed the trend: PTFE-100 > PVDF-100 > PES-90, likely due to the hydrophobicity of the supports. The hydrophobic PDMS layer or silica nanoparticles had a stronger affinity for the hydrophobic PTFE membrane compared to the more hydrophilic PVDF and PES membranes. Mass retention also reflected this trend, with the PTFE membrane retaining 93.0% of the PDMS coating, while PVDF and PES retained only 42.5% and 14.1%, indicating insufficient affinity with the PDMS coating. Varying the nominal pore size of the PTFE support showed an increase in coating efficiency from 50 to 100 nm, with a slight decrease at 450 nm. However, mass residual remained relatively stable across different pore sizes, ranging from 93.0% for PTFE-100 to 89.8% for PTFE-450.

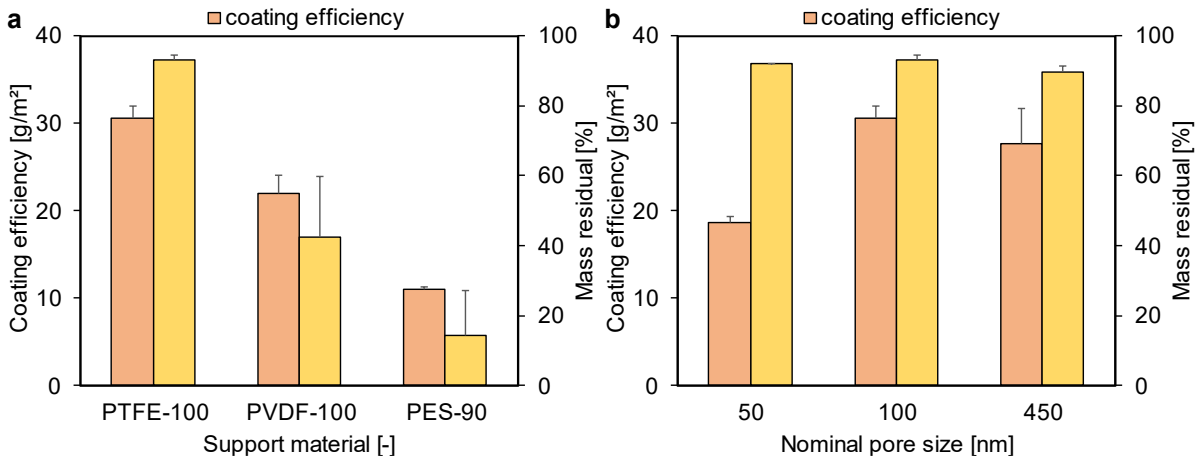

Figure 11. Experimental results of the coating efficiency and mass residual for (a) various support materials, and (b) PTFE membranes with various pore sizes, after a 30 min PDMS coating.

3.2.2 SLM extraction performance

SLM extraction performance was evaluated by measuring the solute fluxes of the amines and the selectivity of the target amines MBA and MPPA over the donor amine IPA, as can be seen in Figure 12. Compared to the pristine PTFE membrane impregnated with the ionic liquid $[P_{6,6,6,14}][N(Tf)_2]$, the membrane with silica nanoparticle addition showed a decrease in the solute fluxes of MBA and MPPA, with an outlier observed for IPA. In contrast, the PDMS-coated membrane exhibited much higher MBA and MPPA fluxes, with a similar IPA flux as the IL-wetted membrane, leading to improved selectivity compared to the IL benchmark (see Figure 12b). Therefore, tight ME with PDMS coating outperformed open ME with IL impregnation, which is consistent with other findings [52].

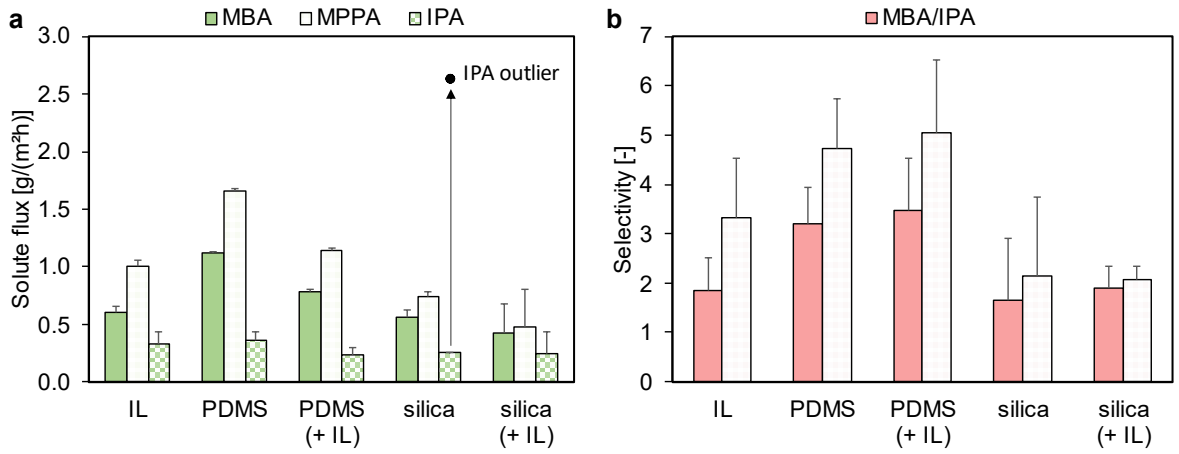

Figure 12. Experimental results of (a) the average solute fluxes, and (b) the selectivity for membrane extraction using a pristine PTFE-100 membrane impregnated with $[P_{6,6,6,14}][N(Tf)_2]$ and/or coated with silica nanoparticles or PDMS.

When the PDMS-coated or silica-coated membranes were impregnated with the IL, a significant reduction in flux was observed (see Figure 12a). This decline is likely due to the higher viscosity of the IL, which slows down solute diffusion. Additionally, the selectivity of the PDMS-coated membrane showed only a slight improvement after IL impregnation. It is important to note that the ionic liquid $[P_{6,6,6,14}][N(Tf)_2]$ raises safety concerns, as it is flammable and corrosive (according to supplier data). In contrast, tight PDMS coatings offer a safer and more environmentally friendly alternative, with low toxicity and no bioaccumulation, making them preferable to open ME systems with IL extractants [53].

To further enhance the extraction performance, the pore size of the support material was varied. As shown in Figure 13, increasing the pore size resulted in a notable decrease in both solute fluxes and selectivity. A larger pore size improved coating efficiency (refer to Figure 11b) by facilitating PDMS penetration into the support matrix. However, the main reason for the flux decline is likely the larger

thickness of the support material with larger pore sizes, which lengthens the diffusion path and negatively affects both fluxes and selectivity [37]. In conclusion, tight ME using a dense PDMS layer combined with a support material of small pore size outperformed both open ME and the combined coating/IL approach in terms of solute flux, selectivity, and stability. The PDMS-coated membrane demonstrated superior flux and performance, offering enhanced safety benefits. A comparison with literature data is presented in Table S1. While undecane achieves the highest MBA flux, it was previously reported as unstable [36]. This study highlights that the non-toxic PDMS-coating provides high stability and achieves a flux exceeding that of the IL-wetted membrane. Variations in flux data may arise from differing experimental conditions, such as operating temperature and feed concentration. Nonetheless, this study demonstrates a significant improvement in flux and stability, compared to the literature data.

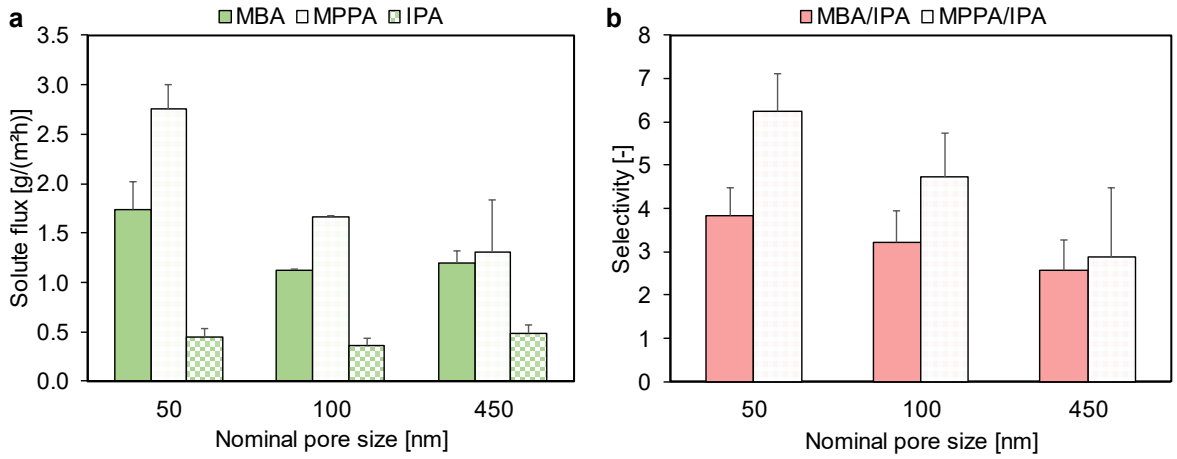

Figure 13. Experimental results of (a) the average solute fluxes, and (b) the selectivity for membrane extraction using a PDMS-coated PTFE-100 membrane with various pore sizes.

4 Conclusion

This study explored novel strategies for enhancing the performance of supported liquid membranes (SLMs) in the selective separation of the aromatic amines α-methylbenzylamine (MBA) and 1-methyl-3-phenylpropylamine (MPPA) from isopropyl amine (IPA). Specifically, various commercial support materials with varying pore sizes were modified by the addition of hydrophobic silica nanoparticles or a polydimethylsiloxane (PDMS) coating. The modified membranes were then characterized and tested in both an open and tight ME configuration, *i.e.*, with or without the addition of an ionic liquid extractant.

FTIR analysis confirmed the successful application of PDMS and silica coatings on all considered support materials. SEM-EDS analysis revealed that PDMS formed a dense and uniform layer, while silica nanoparticles created a porous, fibrous structure. The coating time had little to no impact on the PDMS layer, which consistently covered the internal membrane structure. The addition of silica nanoparticles enhanced hydrophobicity, achieving water contact angles of 124-134°, while PDMS coatings provided a consistent wettability range of 91-100°. Ionic liquid impregnation reduced the water contact angle to 97° and 98° for the silica nanoparticle-coated and PDMS-coated membranes, respectively, indicating better compatibility with the PDMS coating.

The coating efficiency for both silica nanoparticle and PDMS coatings was similar, ranging from 20 to 30 g/m², though silica coatings showed more variability. After membrane extraction testing, the PDMS-coated membranes retained 93.0% of their mass, while the silica-coated membranes retained only 51.3%, indicating that PDMS coatings outperformed silica nanoparticles considerably. The support material significantly impacted the PDMS coating, with coating efficiency and mass retention decreasing in the order: PTFE-100 > PVDF-100 > PES-90, indicating a stronger PDMS affinity for more hydrophobic supports, such as PTFE. The PDMS coating maintained stable mass retention across varying pore sizes (100 to 450 nm), highlighting its compatibility and consistent performance.

The membrane extraction performance was assessed based on solute fluxes and selectivity for MBA/IPA and MPPA/IPA, comparing tight and open ME systems. Tight PDMS-coated membranes outperformed open ionic liquid (IL)-wetted membranes, delivering higher fluxes and improved selectivity while avoiding safety concerns associated with ILs. PDMS coatings offer a safer, more environmentally friendly alternative by reducing concerns related to the flammability and corrosiveness of ILs. This study emphasizes the advantages of PDMS in tight ME configurations, showcasing its low toxicity, stable performance, and minimal environmental impact. Future research should focus on exploring the reusability, long-term stability, and industrial scalability of PDMS-coated membranes, as well as integrating sustainable coating materials for further performance enhancement.

Acknowledgement

The authors would like to acknowledge the Flemish Strategic Basic Research Program of the Catalisti cluster and Flanders Innovation & Entrepreneurship for the financial support provided through the EASiCHEM project (contracts HBC.2018.0484 and K200522N). Additionally, the authors acknowledge the support provided by the Scientific and Technological Research Council of Turkey (TUBITAK)-2219 through the International Postdoctoral Research Fellowship Program, and the National Council of Science and Technology (CONACyT) in Mexico through the PhD scholarship “Estudios de Doctorado en el Extranjero” (contract 2020-000000-01EXT-00130).

Conflict of interest statement

The authors declare that there is no conflict of interest.

Declaration of generative AI and AI-assisted technologies in the writing process

During the preparation of this work the authors used ChatGPT, developed by OpenAI, in order to assist in drafting and refining this manuscript. After using this tool/service, the authors reviewed and edited the content as needed and take full responsibility for the content of the publication.

References

[1] A. Cabré, X. Verdaguer, A. Riera, Recent advances in the enantioselective synthesis of chiral amines via transition metal-catalyzed asymmetric hydrogenation, Chem Rev, 122 (2022) 269–339.

[2] K. Wang, J. Yin, J. Chen, J. Ma, H. Si, D. Xia, Inhibition of inflammation by berberine: Molecular mechanism and network pharmacology analysis, Phytomedicine, 128 (2024) 155258.

[3] Y. Ma, C. Li, F. Han, Y. Liu, U.E. Hani, Y. Zhong, D. Huang, W. Chen, H. Qian, Oral delivery of berberine by liver-targeted zwitterionic nanoparticles to overcome multi-intestinal barriers and extend insulin treatment duration, Chemical Engineering Journal, 485 (2024) 150129.

[4] F.Y. Zhu, M.Y. Huang, K. Zheng, X.J. Zhang, X. Cai, L.G. Huang, Z.Q. Liu, Y.G. Zheng, Designing a novel (R)-ω-transaminase for asymmetric synthesis of sitagliptin intermediate via motif swapping and semi-rational design, Int J Biol Macromol, 253 (2023) 127348.

[5] J.K. Ho, M. Shaker, M. Greenhawt, M. Sadatsafavi, E.M. Abrams, J. Oppenheimer, G.S. Mosnaim, T.Y. Lee, K.M. Johnson, Cost-effectiveness of budesonide-formoterol vs inhaled epinephrine in US adults with mild asthma, Annals of Allergy, Asthma and Immunology, 132 (2024) 229–239.

[6] J. Brousseau, A. Xolin, L. Barriault, A Nine-Step Formal Synthesis of (±)-Morphine, Org Lett, 21 (2019) 1347–1349.

[7] S.K. Singh, P. Gogoi, A. Deb, P.S. Gooh Pattader, Chiral resolution of racemic amines in μ-reactor-crystallizer, Chem Eng Sci, 256 (2022) 117686.

[8] M. Rueping, J. Dufour, F.R. Schoepke, Advances in catalytic metal-free reductions: From bio-inspired concepts to applications in the organocatalytic synthesis of pharmaceuticals and natural products, Green Chemistry, 13 (2011) 1084–1105.

[9] J. Wang, Y.-G. Zhou, Organocatalytic Transfer Hydrogenation, in: Homogeneous Hydrogenation with Non-Precious Catalysts, John Wiley & Sons Ltd, 2019: pp. 261–284.

[10] J. Liu, W. Kong, J. Bai, Y. Li, L. Dong, L. Zhou, Y. Liu, J. Gao, R.T. Bradshaw Allen, N.J. Turner, Y. Jiang, Amine dehydrogenases: Current status and potential value for chiral amine synthesis, Chem Catalysis, 2 (2022) 1288–1314.

[11] M.D. Patil, G. Grogan, A. Bommarius, H. Yun, Oxidoreductase-Catalyzed Synthesis of Chiral Amines, ACS Catal, 8 (2018) 10985–11015.

[12] W. Khanam, N.C. Dubey, Recent advances in immobilized ω-transaminase for chiral amine synthesis, Mater Today Chem, 24 (2022) 100922.

[13] D. Koszelewski, K. Tauber, K. Faber, W. Kroutil, ω-Transaminases for the synthesis of non-racemic α-chiral primary amines, Trends Biotechnol, 28 (2010) 324–332.

[14] G. Van Eygen, D. Mariën, A. Vananroye, C. Clasen, B. Van der Bruggen, A. Buekenhoudt, J.A.P. Coutinho, P. Luis, Facilitated solvent screening for membrane-based extraction of chiral amines via a priori simulations, J Mol Liq, 375 (2023) 121351.

[15] A. Freeman, J.M. Woodley, M.D. Lilly, In Situ Product Removal as a Tool for Bioprocessing, 1993.

[16] A.G. Santos, T.L. de Albuquerque, B.D. Ribeiro, M.A.Z. Coelho, In situ product recovery techniques aiming to obtain biotechnological products: A glance to current knowledge, Biotechnol Appl Biochem, 68 (2021) 1044–1057.

[17] D. Bitas, V. Samanidou, A. Kabir, R. Lucena, S. Cárdenas, 9 - Membrane sorptive phases, in: Analytical Sample Preparation With Nano- and Other High-Performance Materials, Elsevier, 2021: pp. 199–228.

[18] L. Chimuka, E. Cukrowska, J.Å. Jönsson, Why liquid membrane extraction is an attractive alternative in sample preparation*, 2004.

[19] M. Teramoto, H. Tanimoto, Mechanism of Copper Permeation through Hollow Fiber Liquid Membranes, Sep Sci Technol, 18 (1983) 871–892.

[20] M. Teramoto, Y. Sakaida, S. Fu, N. Ohnishi, H. Matsuyama, T. Maki, T. Fukui, K. Arai, An attempt for the stabilization of supported liquid membrane, 2000.

[21] W. Liu, L. He, M. Wang, L. Wei, L. Xu, Z. Zhou, Z. Ren, Effective removal of ammonia from wastewater using hollow fiber renewal liquid membrane, Asia-Pacific Journal of Chemical Engineering, 13 (2018) e2245.

[22] Z. Ren, W. Zhang, Y. Lv, J. Li, Simultaneous extraction and concentration of penicillin G by hollow fiber renewal liquid membrane, Biotechnol Prog, 25 (2009) 468–475.

[23] S.A. Allahyari, A. Minuchehr, S.J. Ahmadi, A. Charkhi, Thorium pertraction through hollow fiber renewal liquid membrane (HFRLM) using Cyanex 272 as carrier, Progress in Nuclear Energy, 100 (2017) 209–220.

[24] X. Fan, S. Liu, Z. Jia, J.J. Koh, J.C.C. Yeo, C.G. Wang, N.E. Surat'man, X.J. Loh, J. Le Bideau, C. He, Z. Li, T.P. Loh, Ionogels: recent advances in design, material properties and emerging biomedical applications, Chem Soc Rev, 52 (2023) 2497–2527.

[25] L. Zhang, D. Jiang, T. Dong, R. Das, D. Pan, C. Sun, Z. Wu, Q. Zhang, C. Liu, Z. Guo, Overview of Ionogels in Flexible Electronics, Chemical Record, (2020).

[26] M.A. Kuzina, D.D. Kartsev, A. V. Stratonovich, P.A. Levkin, Organogels versus Hydrogels: Advantages, Challenges, and Applications, Adv Funct Mater, 33 (2023).

[27] H.R. Mahdavi, M. Arzani, M. Isanejad, T. Mohammadi, Effect of hydrophobic and hydrophilic nanoparticles loaded in D2EHPA/M2EHPA - PTFE supported liquid membrane for simultaneous cationic dyes pertraction, J Environ Manage, 213 (2018) 288–296.

[28] M. Zarak, S. Atif, X. Meng, M. Tian, Enhancing interfacial interaction of PDMS matrix with ZIF-8 via embedding TiO2@ZIF-8 composites for phenol extraction in aqueous-aqueous membrane extractive process, Chemical Engineering Research and Design, 183 (2022) 546–556.

[29] X. Ren, Y. Jia, X. Lu, T. Shi, S. Ma, Preparation and characterization of PDMS-D2EHPA extraction gel membrane for metal ions extraction and stability enhancement, J Memb Sci, 559 (2018) 159–169.

[30] A.J.B. Kemperman, H.H.M. Rolevink, T. Van Den Boomgaard, H. Strathmann, Hollow-fiber-supported liquid membranes with improved stability for nitrate removal, 1997.

[31] H. Wang, J. Fang, T. Cheng, J. Ding, L. Qu, L. Dai, X. Wang, T. Lin, One-step coating of fluoro-containing silica nanoparticles for universal generation of surface superhydrophobicity, Chemical Communications, (2008) 877–879.

[32] G. Van Eygen, B. Van der Bruggen, A. Buekenhoudt, P. Luis Alconero, Efficient membrane-based affinity separations for chemical applications: A review, Chemical Engineering and Processing - Process Intensification, 169 (2021).

[33] Z. Zhao, M. Liao, G. Hu, S. Zeng, L. Ge, K. Yang, Enantioselective adsorption of ibuprofen enantiomers using chiral-active carbon nanoparticles induced S-α-methylbenzylamine, Chirality, 36 (2024).

[34] C. Kouklovsky, 316 Synthetically Derived Auxiliaries: Amines (including Diamines), Hydrazines and Hydroxylamines, and Amino Alcohols, in: Comprehensive Chirality, 2012: pp. 486–527.

[35] M.S. Suleman, K.K. Lau, Y.F. Yeong, Enhanced gas separation performance of PSF membrane after modification to PSF/PDMS composite membrane in CO2/CH4 separation, J Appl Polym Sci, 135 (2018).

[36] G. Van Eygen, D. Mariën, A. Vananroye, C. Clasen, B. Van der Bruggen, A. Buekenhoudt, J.A.P. Coutinho, P. Luis, Facilitated solvent screening for membrane-based extraction of chiral amines via a priori simulations, J Mol Liq, 375 (2023) 121351.

[37] G. Van Eygen, S. Keuppens, X. De Breuck, B. Swankaert, P. Boura, E. Loccufier, J. Kosek, D. Ramasamy, F. Nahra, A. Buekenhoudt, K. De Clerck, B. Van der Bruggen, P. Luis, Comparison of distinctive polymeric membrane structures as support materials for membrane extraction of chiral amines, Sep Purif Technol, 352 (2025).

[38] W. Riedl, Membrane-Supported Liquid-Liquid Extraction – Where Do We Stand Today?, ChemBioEng Reviews, 8 (2021) 6–14.

[39] P.K. Parhi, Supported liquid membrane principle and its practices: A short review, J Chem, 2013 (2013).

[40] S. Hamouni, O. Arous, D. Abdessemed, G. Nezzal, B. Van der Bruggen, Alcohol and alkane organic extraction using pervaporation process, Macromol Symp, 386 (2019).

[41] L. Jiang, M. Gong, J. Sun, Y. Lin, K. Tu, Y. Chen, T. Xiao, X. Li, X. Tan, The design and performance research of PTFE/PVDF/PDMS superhydrophobic radiative cooling composite coating with high infrared emissivity, Mater Today Commun, 38 (2024).

[42] M. Pyo, S. Jeong, J.H. Kim, M.J. Jeon, E.J. Lee, Hydrophobicity and membrane distillation performance of glass fiber membranes modified by dip coating of pure PDMS, J Environ Chem Eng, 12 (2024).

[43] Q. Liu, X. Liu, B. Wu, C. Wang, T. Li, W. Li, Y. Huang, Y. Li, H. Yan, C. Li, Structure regulation of PDMS coating on PTFE membrane surface to achieve efficient separation of gaseous peppermint aromatic water, Appl Surf Sci, 665 (2024).

[44] D. Li, F. Yang, X. Shi, S. Ning, Z. Guo, Utilizing a layer-by-layer self-assembly strategy to construct eco-friendly and sustainable superhydrophobic C–S@PDMS@SiO2 coatings on engineering materials for efficient oil-water separation, Materials Today Sustainability, 27 (2024).

[45] R. Tian, X. Du, Q. Guo, Y. Li, P. Zhang, K. Chen, X. Li, Q. Huang, A simple and efficient approach for pore structure optimization and hydrophilic modification of PTFE nanofiber membrane, Sep Purif Technol, 354 (2025).

[46] Q. He, W. Chen, P. Wang, X. Dou, Silicalite-1/PDMS hybrid membranes on porous PVDF supports: Preparation, structure and pervaporation separation of dichlorobenzene isomers, Polymers (Basel), 14 (2022).

[47] H. Feng, H. Li, M. Li, X. Zhang, Construction of omniphobic PVDF membranes for membrane distillation: Investigating the role of dimension, morphology, and coating technology of silica nanoparticles, Desalination, 525 (2022).

[48] L.W. McKeen, Chapter 4 Binders, in: Fluorinated Coatings and Finishes Handbook, Norwich, NY, 2015: pp. 45–58.

[49] A.W. Mohammad, Y.H. Teow, W.C. Chong, K.C. Ho, Chapter 13 - Hybrid processes: Membrane Bioreactor, in: Membrane Separation Principles and Applications, Elsevier, 2019: pp. 401–470.

[50] Q. Guo, Y. Huang, M. Xu, Q. Huang, J. Cheng, S. Yu, Y. Zhang, C. Xiao, PTFE porous membrane technology: A comprehensive review, J Memb Sci, 664 (2022).

[51] L.L. Radulovic, Z.W. Wojcinski, PTFE (Polytetrafluoroethylene; Teflon®), in: P. Wexler (Ed.), Encyclopedia of Toxicology, 3rd ed., Academix Press, Oxford, 2014: pp. 1133–1136.

[52] S. Salvador Cob, K. De Sitter, A. Buekenhoudt, Application of tight membrane extraction as an in-situ product recovery technology in chiral amine synthesis, Submitted, (n.d.).

[53] E.J. Hobbs, M.L. Keplinger, J.C. Calandra, Toxicity of polydimethylsiloxanes in certain environmental systems, Environ Res, 10 (1975) 397–406.